Refined saddle-point preconditioners for discretized Stokes problems

Pearson, John and Pestana, Jennifer and Silvester, David

2016

MIMS EPrint: **2016.5**

Manchester Institute for Mathematical Sciences
School of Mathematics

The University of Manchester

Reports available from: http://eprints.maths.manchester.ac.uk/
And by contacting: The MIMS Secretary
School of Mathematics
The University of Manchester
Manchester, M13 9PL, UK

ISSN 1749-9097

REFINED SADDLE-POINT PRECONDITIONERS FOR DISCRETIZED STOKES PROBLEMS

JOHN W. PEARSON*, JENNIFER PESTANA†, AND DAVID J. SILVESTER‡

Abstract. This paper is concerned with the implementation of efficient solution algorithms for elliptic problems with constraints. We establish theory which shows that including a simple scaling within well-established block diagonal preconditioners for Stokes problems can result in significantly faster convergence when applying the preconditioned MINRES method. The codes used in the numerical studies are available online.

Key words. Stokes equations, stabilization, saddle-point systems, preconditioning, inf–sup condition

AMS subject classifications. 65F10, 65F15, 65N30

1. Introduction. The motivation for this work is the development of fast and robust linear solvers for stabilized mixed approximations of the Stokes equations,

$$\begin{aligned} -\nabla^2 \vec{v} + \nabla p &= \vec{f}, \\ -\nabla \cdot \vec{v} &= 0, \end{aligned}$$

together with suitable (Dirichlet, Neumann or mixed) boundary conditions. Stokes problems typically arise when modelling the flow of a slow-moving fluid such as magma in the Earth's mantle, see [16]. In our setting $\vec{v}$ denotes the flow velocity, p is the pressure, and $\vec{f}$ represents a source term that drives the PDE system. The associated boundary value problem is usually posed on a bounded domain $\Omega \subset \mathbb{R}^d$, $d \in \{2, 3\}$. Stokes problems also arise in a natural way when the (unsteady) Navier–Stokes equations are simplified using classical operator splitting techniques, see [5].

We suppose that the boundary value problem is discretized using standard mixed finite elements. That is we take $\{\phi_i\}_{i=1,\ldots,n_v}$ as the finite element basis functions for the velocity components (we assume that the same approximation space is used for each one), and $\{\psi_i\}_{i=1,\ldots,n_p}$ for the pressure; so that n_v and n_p are the number of velocity and pressure grid nodes respectively. Having set up the associated velocity basis set (for example, $\{\vec{\phi}_1, \ldots, \vec{\phi}_{2n_v}\} := \{(\phi_1, 0)^T, \ldots, (\phi_{n_v}, 0)^T, (0, \phi_1)^T, \ldots, (0, \phi_{n_v})^T\}$ in two dimensions), the resulting discrete Stokes system is the *saddle-point* system,

$$\begin{bmatrix} A & B^T \\ B & -C \end{bmatrix} \begin{bmatrix} \boldsymbol{v} \\ \boldsymbol{p} \end{bmatrix} = \begin{bmatrix} \boldsymbol{f} \\ \boldsymbol{g} \end{bmatrix}, \tag{1.1}$$

where $A \in \mathbb{R}^{dn_v \times dn_v}$ is the *vector-Laplacian matrix* given by

$$A = [a_{ij}], \qquad a_{ij} = \int_\Omega \nabla \vec{\phi}_i : \nabla \vec{\phi}_j \, \mathrm{d}\Omega,$$

and $B \in \mathbb{R}^{n_p \times dn_v}$ is the *divergence matrix*

$$B = [b_{ij}], \qquad b_{ij} = \int_\Omega \psi_i \nabla \cdot \vec{\phi}_j \, \mathrm{d}\Omega.$$

*School of Mathematics, Statistics and Actuarial Science, University of Kent, Cornwallis Building (East), Canterbury, CT2 7NF, United Kingdom (j.w.pearson@kent.ac.uk),

†Department of Mathematics and Statistics, University of Strathclyde, Glasgow, G1 1XH, United Kingdom (jennifer.pestana@strath.ac.uk),

‡School of Mathematics, University of Manchester, Oxford Road, Manchester, M13 9PL, United Kingdom (d.silvester@manchester.ac.uk)

The vectors $\boldsymbol{v}$, $\boldsymbol{p}$ are discretized representations of $\vec{v}$, p, with $\boldsymbol{f}$, $\boldsymbol{g}$ taking into account the source term $\vec{f}$ as well as nonhomogeneous boundary conditions. The matrix C is the zero matrix when a stable finite element discretization (such as the Q_2–Q_1 Taylor–Hood element) is used, and is the *stabilization matrix* otherwise. We assume that A is symmetric positive definite, which is the case when a Dirichlet condition is imposed on at least part of the boundary. The matrix C is always positive semi-definite. For consistency with the continuous Stokes system the matrix B should satisfy $\mathbf{1} \in \text{null}(B^T)$ in the case of enclosed flow (see, e.g., [7, Chapter 3]). However, other vectors may also lie in the nullspace of B; these are artefacts of the discretization, or arise from the imposition of essential boundary conditions.

The matrix system (1.1) is of classical *saddle point form*.[1] There has been a great deal of research devoted to solving systems of the form (1.1) using preconditioned iterative methods; see [2] for a definitive review. This body of work is relevant to any linear system that is generated by a mixed approximation; see [4, Chapter 3] for a characterization. To state the key spectral properties, it is useful to let

$$\mathcal{A} = \begin{bmatrix} A & B^T \\ B & -C \end{bmatrix}, \tag{1.2}$$

where $A \in \mathbb{R}^{n\times n}$ is symmetric positive definite as above, $C \in \mathbb{R}^{m\times m}$ is symmetric positive semidefinite, $B \in \mathbb{R}^{m\times n}$ with $m \leq n$ and $\text{rank}(B) = r \leq m$.[2] We suppose that the (negative) Schur complement of $\mathcal{A}$,

$$S = BA^{-1}B^T + C,$$

has rank p. Then under these conditions $\mathcal{A}$ has n positive eigenvalues, p negative eigenvalues and $m - p$ zero eigenvalues [2, page 21].

A widely studied block diagonal preconditioner for $\mathcal{A}$ is given by

$$\mathcal{P}_1 = \begin{bmatrix} A & 0 \\ 0 & H \end{bmatrix}, \tag{1.3}$$

where $H \in \mathbb{R}^{n\times n}$ is some symmetric positive definite approximation to the Schur complement S. In the case where $H = S$ and $C = 0$, it is known that the eigenvalues of the preconditioned system are given by [13, 15]

$$\lambda(\mathcal{P}_1^{-1}\mathcal{A}) \in \left\{1, \frac{1}{2}(1 \pm \sqrt{5})\right\},$$

and in the case where the approximation of S (or indeed A) is inexact the preconditioner is frequently found to be extremely effective also. When the condition on C is weakened to allow the matrix to be symmetric positive semi-definite, it can be shown that[3]

$$\lambda(\mathcal{P}_1^{-1}\mathcal{A}) \in \left[-1, \frac{1}{2}(1 - \sqrt{5})\right] \cup \left[1, \frac{1}{2}(1 + \sqrt{5})\right].$$

[1] We note that the condition $C = 0$ is often required for a matrix to be defined as a saddle-point system. In this work we consider the more general definition, where C is required to be symmetric positive semi-definite.

[2] In the case of the Stokes discretization, $n = dn_v$ and $m = n_p$.

[3] The lower bounds on the positive and negative eigenvalues are shown in [1, Corollary 1], with the upper bounds on the positive and negative eigenvalues a result of [21, Lemma 2.2].

In the specific case of the Stokes equations, the approximate Schur complement H is either the *mass matrix* associated with the pressure approximation space[4]

$$Q = [m_{p,ij}], \qquad m_{p,ij} = \int_\Omega \psi_i \psi_j \, \mathrm{d}\Omega,$$

the diagonal of this matrix (see [21, 24]), a lumped version of Q (see [22]), or a Chebyshev semi-iteration method applied to it (see [11, 12, 26]). We will study a refined version of the classical preconditioner in this work: instead of taking $S \approx H$, our idea is to incorporate a scaling constant $\alpha > 0$ and investigate using

$$\mathcal{P}_\alpha = \begin{bmatrix} A & 0 \\ 0 & \alpha H \end{bmatrix} \tag{1.4}$$

as a potential preconditioner for $\mathcal{A}$. Intuitively there is little reason to assume that the matrix $\mathcal{P}_\alpha$ would be a more effective preconditioner than $\mathcal{P}_1$: by scaling the Schur complement we are after all moving the preconditioner 'further' from the *ideal* preconditioner $\mathcal{P}_1$. Remarkably, however, we frequently observe a significant improvement in the Stokes case. This improvement is justified theoretically herein. We also explain why setting a large value of α can significantly improve the performance of the iterative solver when a stabilized mixed approximation is employed.

2. Generic spectral equivalence bounds. Extensions to existing eigenvalue bounds for the Stokes problem are discussed in this section. We analyse the "ideal" Stokes preconditioner (1.4) first, but we also discuss bounds for efficient "inexact" variants. These results provide informal motivation for modifying the standard saddle-point preconditioner for the Stokes equations. Refined eigenvalue estimates applicable in a Stokes setting are presented in Section 3.

To fix ideas, we characterize the eigenvalues of $\mathcal{P}_\alpha^{-1}\mathcal{A}$ using the following theorem. Although the result is simple, and is similar in flavour to results in many other papers (e.g., [3, 10, 17, 21]), it forms the basis of our analysis and so we provide a proof for completeness. We highlight that this corresponds to an exact application of the $(1,1)$-block A within the preconditioner. From now on we use the notation (F, G) to denote the generalized eigenvalue problem $F\boldsymbol{v} = \lambda G\boldsymbol{v}$.

THEOREM 2.1. *Consider the generalized eigenvalue problem*

$$\mathcal{A}\begin{bmatrix} \boldsymbol{x} \\ \boldsymbol{y} \end{bmatrix} = \lambda \mathcal{P}_\alpha \begin{bmatrix} \boldsymbol{x} \\ \boldsymbol{y} \end{bmatrix}, \tag{2.1}$$

where $\mathcal{A}$, $\mathcal{P}_\alpha$ are as in (1.2), (1.4). *We have* $\operatorname{rank}(B) = r \leq m$, $\lambda \in \mathbb{R}$, $\boldsymbol{x} \in \mathbb{R}^n$ *and* $\boldsymbol{y} \in \mathbb{R}^m$, *with $\boldsymbol{x}$ and $\boldsymbol{y}$ not simultaneously zero vectors. Then,*

I. $\lambda = 1$ *with multiplicity* $n - r$, *with associated eigenvectors* $[\boldsymbol{x}^T, \boldsymbol{0}^T]^T$, $\boldsymbol{x} \in \operatorname{null}(B)$;

II. λ *satisfies* $-C\boldsymbol{y} = \lambda\alpha H\boldsymbol{y}$ *with* $\boldsymbol{y} \in \operatorname{null}(B^T)$, *in which case the associated eigenvector of* $(\mathcal{A}, \mathcal{P}_\alpha)$ *is* $[\boldsymbol{0}^T, \boldsymbol{y}^T]^T$;

III. *or* $\lambda = \frac{1}{2}(1-\gamma) \pm \frac{1}{2}\sqrt{(1-\gamma)^2 + 4\delta}$, *where* $\gamma = \boldsymbol{y}^T C\boldsymbol{y}/\boldsymbol{y}^T\alpha H\boldsymbol{y} \geq 0$ *and* $\delta = \boldsymbol{y}^T(BA^{-1}B^T + C)\boldsymbol{y}/\boldsymbol{y}^T\alpha H\boldsymbol{y} > 0$, *with* $\boldsymbol{x} \neq \boldsymbol{0}$, $\boldsymbol{y} \notin \operatorname{null}(B^T)$.

[4] This follows from expressing the discrete inf-sup stability condition as a generalized eigenvalue problem, see [7, page 173].

Proof. Equation (2.1) is equivalent to

$$B^T\boldsymbol{y} = (\lambda - 1)A\boldsymbol{x} \tag{2.2}$$

$$B\boldsymbol{x} = (\lambda\alpha H + C)\boldsymbol{y}. \tag{2.3}$$

We consider Cases I–III separately.

Case I: If $\lambda = 1$ then (2.2) implies that $B^T\boldsymbol{y} = \boldsymbol{0}$, so either $\boldsymbol{y} = \boldsymbol{0}$ or $\boldsymbol{y} \in \text{null}(B^T)$, $\boldsymbol{y} \neq \boldsymbol{0}$. If $\boldsymbol{y} = \boldsymbol{0}$ then (2.3) implies that $B\boldsymbol{x} = \boldsymbol{0}$, so that $\boldsymbol{x} \in \text{null}(B)$. There are $n - r$ linearly independent such vectors. Otherwise, $\boldsymbol{y} \in \text{null}(B^T)$ with $\boldsymbol{y} \neq \boldsymbol{0}$. However, premultiplying (2.3) by $\boldsymbol{y}^T$ then gives that $\alpha\boldsymbol{y}^T H\boldsymbol{y} = -\boldsymbol{y}^T C\boldsymbol{y}$. Since H is positive definite, C is semidefinite and $\alpha > 0$, this cannot hold. Thus, if $\lambda = 1$ then $\boldsymbol{y} = \boldsymbol{0}$. On the other hand, if $\boldsymbol{y} = \boldsymbol{0}$ we know from (2.2) that $\lambda = 1$, since $\boldsymbol{x} \neq \boldsymbol{0}$ and A is positive definite, so $\lambda = 1$ if and only if $\boldsymbol{y} = \boldsymbol{0}$. Accordingly, 1 is an eigenvalue of $(\mathcal{A}, \mathcal{P}_\alpha)$ with multiplicity $n - r$ and eigenvectors $[\boldsymbol{x}^T, \boldsymbol{0}^T]^T$, $\boldsymbol{x} \in \text{null}(B)$.

Case II: We now assume that $\boldsymbol{y} \in \text{null}(B^T)$, $\boldsymbol{y} \neq \boldsymbol{0}$. From Case I we know that this implies that $\lambda \neq 1$. Then, (2.2) shows that $\boldsymbol{x} = \boldsymbol{0}$. From (2.3) it follows that λ and $\boldsymbol{y}$ satisfy the generalized eigenvalue problem $-C\boldsymbol{y} = \lambda\alpha H\boldsymbol{y}$. Thus $\boldsymbol{y}$ must simultaneously be an eigenvector of $(-C, \alpha H)$ and in the nullspace of B^T. Note that at most $m - r$ linearly independent vectors satisfy this requirement.

Case III: Otherwise, we know that $\lambda \neq 1$, $\boldsymbol{x} \neq \boldsymbol{0}$, $\boldsymbol{y} \notin \text{null}(B^T)$. We can rearrange (2.2) for $\boldsymbol{x}$ and substitute into (2.3) to give

$$\frac{1}{\lambda - 1} BA^{-1}B^T\boldsymbol{y} = (\lambda\alpha H + C)\boldsymbol{y}$$

or $\lambda^2 - (1 - \gamma)\lambda - \delta = 0$, the solution of which is

$$\lambda = \frac{1}{2}(1 - \gamma) \pm \frac{1}{2}\sqrt{(1 - \gamma)^2 + 4\delta}$$

as required. □

We see that it is possible to describe the eigenvalues of $\mathcal{P}_\alpha^{-1}\mathcal{A}$ in terms of A, B, C, H and α. We also note that when $C = 0$ (as arises when solving the Stokes equations using stable finite elements), Case II does not occur and Case III describes all eigenvalues not equal to 1.

This is a good place to pause to consider the implications of Theorem 2.1 and the effect of scaling $\mathcal{P}_\alpha$ on the eigenvalues of the preconditioned matrix. Trivially, eigenvalues satisfying Case I are positive (since $\lambda = 1$) while any eigenvalues satisfying Case II are negative, since C is semidefinite and H is positive definite. The remaining eigenvalues of $\mathcal{P}_\alpha^{-1}\mathcal{A}$ may be positive, negative or zero and the inertia of $\mathcal{P}_\alpha^{-1}\mathcal{A}$ must be the same as that of $\mathcal{A}$. However, because C is semidefinite and A and H are positive definite, any positive eigenvalue must be at least one, and approaches one as α increases. On the other hand, negative eigenvalues may approach zero from below, as α increases, which can have a detrimental affect on the speed of convergence of preconditioned MINRES. For this reason, it is interesting and important to examine in greater detail the effect of α on the eigenvalues of $\mathcal{P}_\alpha^{-1}\mathcal{A}$.

In the case of the Stokes equations, an effective preconditioner will not invert the $(1, 1)$-block exactly as this will be very expensive computationally. However it is reasonable to assume, as in [21], that an approximation $\widehat{A}$ may be constructed such that

$$g(h) \leq \frac{\boldsymbol{v}^T A\boldsymbol{v}}{\boldsymbol{v}^T \widehat{A}\boldsymbol{v}} \leq 1, \qquad \forall \boldsymbol{v} \in \mathbb{R}^n \backslash \{\boldsymbol{0}\}, \tag{2.4}$$

for some function g of the mesh parameter h. Applying a tailored multigrid method to approximate the action of A^{-1}, for example, will achieve this property with $g(h)$ bounded away from zero independently of h. For stable finite element discretizations of the Stokes equation there exists an inf-sup constant γ, and a constant Γ resulting from the boundedness of B, such that

$$\gamma^2 \leq \frac{\boldsymbol{p}^T B A^{-1} B^T \boldsymbol{p}}{\boldsymbol{p}^T Q \boldsymbol{p}} \leq \Gamma^2, \qquad \forall \boldsymbol{p} \in \mathbb{R}^m \backslash \{\mathbf{0}\}. \tag{2.5}$$

For an unstable discretization only the upper bound holds, and a lower bound is assumed as follows:

$$\gamma^2 \leq \frac{\boldsymbol{p}^T (B A^{-1} B^T + C) \boldsymbol{p}}{\boldsymbol{p}^T Q \boldsymbol{p}}, \qquad \frac{\boldsymbol{p}^T B A^{-1} B^T \boldsymbol{p}}{\boldsymbol{p}^T Q \boldsymbol{p}} \leq \Gamma^2, \qquad \forall \boldsymbol{p} \in \mathbb{R}^m \backslash \{\mathbf{0}\}. \tag{2.6}$$

Furthermore we assume that there exist mesh-independent constants θ, Θ guaranteeing the spectral equivalence of Q and our Schur complement approximation H, that is:

$$\theta^2 \leq \frac{\boldsymbol{p}^T Q \boldsymbol{p}}{\boldsymbol{p}^T H \boldsymbol{p}} \leq \Theta^2, \qquad \forall \boldsymbol{p} \in \mathbb{R}^m \backslash \{\mathbf{0}\}. \tag{2.7}$$

Finally we use the boundedness of C to write

$$\frac{\boldsymbol{p}^T C \boldsymbol{p}}{\boldsymbol{p}^T H \boldsymbol{p}} \leq \Delta, \qquad \forall \boldsymbol{p} \in \mathbb{R}^m \backslash \{\mathbf{0}\}, \tag{2.8}$$

for some mesh-independent constant Δ. The properties assumed above all hold for the discretizations and approximations we use in this work. We are now in a position to recall Theorem 2.2 of [21] which in turn provides a bound for the convergence of preconditioned MINRES, see [25, Theorem 4.1].

THEOREM 2.2. *For a stable or stabilized discrete Stokes problem* (1.1) *on a quasi-uniform sequence of grids, assume that* (2.4) *holds with* $g(h) \to 0$ *as* $h \to 0$*, that* (2.5) *or* (2.6) *holds, and that* (2.7), (2.8) *are satisfied. Then the eigenvalues of the preconditioned system* $\widehat{\mathcal{P}}_1^{-1}\mathcal{A}$*, where*

$$\widehat{\mathcal{P}}_1 = \begin{bmatrix} \widehat{A} & 0 \\ 0 & H \end{bmatrix},$$

satisfy

$$\begin{aligned} \lambda(\widehat{\mathcal{P}}_1^{-1}\mathcal{A}) \in & \left[-\Delta/2 - \sqrt{\Delta^2/4 + \Gamma^2\Theta^2} + \mathcal{O}(g(h)), -\gamma\theta\sqrt{g(h)} + \mathcal{O}(g(h)) \right] \\ & \cup \left[g(h), 1/2 + \sqrt{1/4 + \Gamma^2\Theta^2} \right]. \end{aligned}$$

The asymptotic convergence rate of preconditioned MINRES is given by

$$\lim_{k\to\infty} e_k^{1/k} = 1 - g(h)^{3/4} \sqrt{\frac{4\gamma\theta}{\left(\Delta + \sqrt{\Delta^2 + 4\Gamma^2\Theta^2}\right)\left(1 + \sqrt{1 + 4\Gamma^2\Theta^2}\right)}} + \mathcal{O}(g(h)^{5/4}). \tag{2.9}$$

We refer to [25] for discussion of the asymptotic convergence rate for such problems, and to [23, Chapter 3.2] for a definition and motivation of this quantity. From (2.9), we observe that the quantity controlling the 'average' convergence of the method is

$$\mathcal{R}_1 := \frac{4\gamma\theta}{\left(\Delta + \sqrt{\Delta^2 + 4\Gamma^2\Theta^2}\right)\left(1 + \sqrt{1 + 4\Gamma^2\Theta^2}\right)}.$$

That is, if $\mathcal{R}_1$ is maximized, then the 'best' average convergence is achieved. We note that $\Delta = 0$ when no stabilization is applied.

Let us now consider the result of applying the scaled preconditioner given by

$$\widehat{\mathcal{P}}_\alpha = \begin{bmatrix} \widehat{A} & 0 \\ 0 & \alpha H \end{bmatrix}.$$

Then within our assumptions (2.7), (2.8) for Theorem 2.2, we must replace θ^2, Θ^2, Δ with θ^2/α, Θ^2/α, Δ/α, in which case the asymptotic convergence rate becomes

$$\mathcal{R}_\alpha := \frac{\dfrac{4\gamma\theta}{\sqrt{\alpha}}}{\left(\dfrac{\Delta}{\alpha} + \sqrt{\dfrac{\Delta^2}{\alpha^2} + \dfrac{4\Gamma^2\Theta^2}{\alpha}}\right)\left(1 + \sqrt{1 + \dfrac{4\Gamma^2\Theta^2}{\alpha}}\right)}.$$

We now examine the behavior of $\mathcal{R}_\alpha$ as $\alpha \uparrow \infty$, starting with the case where a stable discretization is used (i.e. $\Delta = 0$). In this case

$$\mathcal{R}_\alpha = \frac{\dfrac{4\gamma\theta}{\sqrt{\alpha}}}{\dfrac{2\Gamma\Theta}{\sqrt{\alpha}}\left(1 + \sqrt{1 + \dfrac{4\Gamma^2\Theta^2}{\alpha}}\right)} = \frac{\dfrac{2\gamma\theta}{\Gamma\Theta}}{1 + \sqrt{1 + \dfrac{4\Gamma^2\Theta^2}{\alpha}}}$$

$$\uparrow \frac{\gamma\theta}{\Gamma\Theta} \qquad \text{as } \alpha \uparrow \infty.$$

In the case where a stabilized mixed method is used (i.e. $\Delta \neq 0$), we have

$$\begin{aligned}\mathcal{R}_\alpha &= \frac{\dfrac{4\gamma\theta}{\sqrt{\alpha}}}{\left(\dfrac{\Delta}{\alpha} + \sqrt{\dfrac{\Delta^2}{\alpha^2} + \dfrac{4\Gamma^2\Theta^2}{\alpha}}\right)\left(1 + \sqrt{1 + \dfrac{4\Gamma^2\Theta^2}{\alpha}}\right)} \\ &= \frac{4\gamma\theta}{\left(\dfrac{\Delta}{\sqrt{\alpha}} + \sqrt{\dfrac{\Delta^2}{\alpha} + 4\Gamma^2\Theta^2}\right)\left(1 + \sqrt{1 + \dfrac{4\Gamma^2\Theta^2}{\alpha}}\right)} \\ &\uparrow \frac{4\gamma\theta}{2\Gamma\Theta \cdot 2} = \frac{\gamma\theta}{\Gamma\Theta} \qquad \text{as } \alpha \uparrow \infty.\end{aligned}$$

The above discussion indicates that, for both stable and stabilized discretizations, it may be highly advantageous to increase the scaling parameter α in $\mathcal{P}_\alpha$. In particular, increasing α nullifies the effect of the parameter Δ in the expression for the average convergence rate. As $\alpha \uparrow \infty$, the predicted rate tends to $1 - g(h)^{3/4}\sqrt{\gamma\theta/\Gamma\Theta}$. Of

course this argument is a heuristic, as we do not know from this argument how large α must be to result in substantially faster convergence.

The next section of the paper is the new contribution. Concrete eigenvalue bounds for preconditioned systems are derived and these are connected to the convergence observed when solving the system (1.1) with preconditioners $\mathcal{P}_\alpha$ and $\widehat{\mathcal{P}}_\alpha$.

3. Refined estimates for the negative eigenvalues. The bounds in the previous section suggest that large values of α in $\mathcal{P}_\alpha$ will reduce the condition number of $\mathcal{P}_\alpha^{-1}\mathcal{A}$ and hence improve the convergence rate of preconditioned MINRES applied to Stokes problems. Fast convergence of Krylov subspace methods for symmetric indefinite problems is often attributed to nicely distributed eigenvalues, with clustered eigenvalues often sought.[5] Recalling the remarks after Theorem 2.1, we find that positive eigenvalues of $\mathcal{P}_\alpha^{-1}\mathcal{A}$ cluster near one as α increases. Negative eigenvalues also cluster as α increases, but move towards the origin, which can delay the convergence of Krylov subspace methods. Accordingly, it is instructive to more precisely characterize the negative eigenvalues, particularly the eigenvalue nearest the origin.

Let us order the eigenvalues of $\mathcal{P}_\alpha^{-1}\mathcal{A}$ from smallest to largest, so that

$$\lambda_1 \le \cdots \le \lambda_p < 0 < \lambda_{m+1} \le \cdots \le \lambda_{m+n},$$

where $p = \mathrm{rank}(S)$ and S is the negative Schur complement of $\mathcal{A}$. (Recall that $\mathcal{P}_\alpha^{-1}\mathcal{A}$ has $m - p$ zero eigenvalues.)

We will illustrate the actual behavior of the scaled preconditioner $\mathcal{P}_\alpha$, in which the $(1,1)$ block is A and the $(2,2)$ block is either the pressure mass matrix or its diagonal, by considering a two-dimensional Stokes problem defined in a square domain. We note that additional numerical experiments (described in Section 4), that are conducted with A replaced by a single V-cycle of AMG, show that only λ_{m+1}, which takes values between 0.84 and 0.94, changes significantly when this approximation is made. Another option is to replace $\mathrm{diag}(Q)$, the diagonal of the mass matrix, by $\mathrm{lump}(Q)$, the lumped mass matrix whose entries are the row sums of Q, or by a fixed number of iterations of Chebyshev semi-iteration. Both approaches cause λ_1, λ_p, λ_{m+1} and λ_{m+n} to better approximate the values obtained when $H = Q$. The analysis in the rest of this section could easily be applied to lumped mass matrices also.

As a first step we investigate the extreme nonzero eigenvalues λ_1, λ_p, λ_{m+1} and λ_{m+n} of $\mathcal{P}_\alpha^{-1}\mathcal{A}$ as α varies, for a cavity problem discretized by Q_1–Q_1, Q_1–P_0 and Q_2–Q_1 elements. This is a widely considered problem in Stokes flow, which we define on $\Omega = [-1,1]^2$, with $\vec{f} = \vec{0}$ and boundary conditions given by

$$\begin{aligned} v_x = 1 - x^4,\ v_y = 0, &\quad \text{on } [-1,1] \times \{1\}, \\ v_x = v_y = 0, &\quad \text{on } \partial\Omega \backslash \big([-1,1] \times \{1\}\big), \end{aligned}$$

where $\vec{v} = [v_x,\ v_y]^T$. Since the flow is enclosed, the preconditioned system is singular with a single zero eigenvalue that is associated with a zero velocity and a constant pressure vector.

Tables 3.1–3.2 verify the asymptotic results for large α just mentioned. We also note that λ_p approaches the origin algebraically as α is increased. Other interesting trends also emerge. One intriguing feature of Q_1–Q_1 elements is that, when H in $\mathcal{P}_\alpha$ is

[5] Note that, even in exact arithmetic, matrices with tight clusters of eigenvalues do not in general give the same convergence curve as matrices with distinct eigenvalues located at the cluster centres, as discussed by Liesen and Strakoš for the Conjugate Gradient method [14, Section 5.6.5].

TABLE 3.1

Computed extreme eigenvalues of $\mathcal{P}_\alpha^{-1}\mathcal{A}$ for the cavity problem, a mesh parameter of 2^{-5} and $H = \mathrm{diag}(Q)$, the diagonal of the pressure mass matrix.

	Q_1–Q_1				Q_1–P_0				Q_2–Q_1			
α	λ_1	λ_p	λ_{m+1}	λ_{m+n}	λ_1	λ_p	λ_{m+1}	λ_{m+n}	λ_1	λ_p	λ_{m+1}	λ_{m+n}
1	-1.1	-0.25	1	2.1	-1.3	-0.2	1	1.6	-1.1	-0.11	1	2.1
2	-0.67	-0.13	1	1.7	-0.72	-0.11	1	1.4	-0.65	-0.06	1	1.7
3	-0.5	-0.083	1	1.5	-0.5	-0.073	1	1.3	-0.49	-0.041	1	1.5
4	-0.4	-0.063	1	1.4	-0.39	-0.055	1	1.2	-0.39	-0.031	1	1.4
5	-0.33	-0.05	1	1.3	-0.31	-0.045	1	1.2	-0.33	-0.025	1	1.3
6	-0.29	-0.042	1	1.3	-0.27	-0.038	1	1.1	-0.28	-0.021	1	1.3
7	-0.25	-0.036	1	1.3	-0.23	-0.032	1	1.1	-0.25	-0.018	1	1.2
8	-0.23	-0.031	1	1.2	-0.2	-0.028	1	1.1	-0.22	-0.016	1	1.2
9	-0.21	-0.028	1	1.2	-0.18	-0.025	1	1.1	-0.2	-0.014	1	1.2
10	-0.19	-0.025	1	1.2	-0.16	-0.023	1	1.1	-0.18	-0.013	1	1.2
20	-0.1	-0.013	1	1.1	-0.085	-0.012	1	1	-0.099	-0.0063	1	1.1
40	-0.053	-0.0063	1	1.1	-0.043	-0.0058	1	1	-0.051	-0.0032	1	1.1
60	-0.036	-0.0042	1	1	-0.029	-0.0039	1	1	-0.035	-0.0021	1	1
80	-0.027	-0.0031	1	1	-0.022	-0.0029	1	1	-0.026	-0.0016	1	1
100	-0.022	-0.0025	1	1	-0.017	-0.0023	1	1	-0.021	-0.0013	1	1

TABLE 3.2

Computed extreme eigenvalues of $\mathcal{P}_\alpha^{-1}\mathcal{A}$ for the cavity problem, a mesh parameter of 2^{-5} and $H = Q$, the pressure mass matrix.

	Q_1–Q_1				Q_1–P_0				Q_2–Q_1			
α	λ_1	λ_p	λ_{m+1}	λ_{m+n}	λ_1	λ_p	λ_{m+1}	λ_{m+n}	λ_1	λ_p	λ_{m+1}	λ_{m+n}
1	-1.1	-0.19	1	1.6	-1.3	-0.2	1	1.6	-0.62	-0.18	1	1.6
2	-0.55	-0.1	1	1.4	-0.72	-0.11	1	1.4	-0.37	-0.095	1	1.4
3	-0.38	-0.071	1	1.3	-0.5	-0.073	1	1.3	-0.26	-0.065	1	1.3
4	-0.29	-0.054	1	1.2	-0.39	-0.055	1	1.2	-0.21	-0.049	1	1.2
5	-0.23	-0.044	1	1.2	-0.31	-0.045	1	1.2	-0.17	-0.04	1	1.2
6	-0.2	-0.037	1	1.1	-0.27	-0.038	1	1.1	-0.15	-0.033	1	1.1
7	-0.17	-0.032	1	1.1	-0.23	-0.032	1	1.1	-0.13	-0.029	1	1.1
8	-0.15	-0.028	1	1.1	-0.2	-0.028	1	1.1	-0.11	-0.025	1	1.1
9	-0.13	-0.025	1	1.1	-0.18	-0.025	1	1.1	-0.1	-0.023	1	1.1
10	-0.12	-0.022	1	1.1	-0.16	-0.023	1	1.1	-0.092	-0.02	1	1.1
20	-0.061	-0.011	1	1	-0.085	-0.012	1	1	-0.048	-0.01	1	1
40	-0.031	-0.0057	1	1	-0.043	-0.0058	1	1	-0.024	-0.0052	1	1
60	-0.021	-0.0038	1	1	-0.029	-0.0039	1	1	-0.016	-0.0034	1	1
80	-0.015	-0.0028	1	1	-0.022	-0.0029	1	1	-0.012	-0.0026	1	1
100	-0.012	-0.0023	1	1	-0.017	-0.0023	1	1	-0.0099	-0.0021	1	1

the diagonal of the pressure mass matrix, the eigenvalue λ_p seems to be $-0.25/\alpha$. On the other hand, when H is the full pressure mass matrix and α is large the eigenvalue λ_p is almost (although not exactly) the same for all three element types.

Our next task is to develop good bounds for λ_p and explain some of the phenomena we observe, so that we might choose values of α that results in fast convergence of Krylov methods applied to Stokes problems. To do this we examine both Case II and Case III eigenvalues from Theorem 2.1.

3.1. Case III eigenvalues. We begin by studying Case III eigenvalues, which will help us explain why λ_p is similar for different elements when the full pressure mass matrix Q is used for H. In particular, we show that a simple upper bound from [21] on the negative Case III eigenvalues is remarkably tight. Although the analysis we provide is for the situation $H = Q$, we also give numerical results for $H = \mathrm{diag}(Q)$, and note that the extension of the analysis to this case, or to lumped mass matrices,

TABLE 3.3
Values of $\delta_{\min}$ for different problems and element types when the mesh parameter is 2^{-5}.

	Q_1–Q_1	Q_1–P_0	Q_2–Q_1
Regularized cavity	0.2272	0.2339	0.2074
Obstacle	0.0088	0.0087	0.0088

is straightforward albeit less informative.

Recall from Theorem 2.1 that these negative Case III eigenvalues are

$$\lambda = \frac{1}{2}(1-\gamma) - \frac{1}{2}\sqrt{(1-\gamma)^2 + 4\delta},$$

where $\gamma = \boldsymbol{y}^T C\boldsymbol{y}/\boldsymbol{y}^T\alpha H\boldsymbol{y} \geq 0$, $\delta = \boldsymbol{y}^T(BA^{-1}B^T + C)\boldsymbol{y}/\boldsymbol{y}^T\alpha H\boldsymbol{y} > 0$ and $\boldsymbol{y} \notin \text{null}(B^T)$.

Now, λ is a monotonically decreasing function of γ, with $\gamma \in [0,1]$. Since Q_1–Q_1 and Q_1–P_0 elements satisfy the ideal stabilization property (see [7, Section 3.3.2]), $\gamma \leq 1$ for both element types. Additionally, $\gamma = 0$ for Q_2–Q_1 elements (since $C = 0$ for stable elements). Thus, for all three elements we obtain the bound in Lemma 2.3 of [21]:

$$\lambda_p \leq \frac{1}{2} - \frac{1}{2}\sqrt{1 + 4\delta_{\min}}, \tag{3.1}$$

where

$$\delta_{\min} = \min_{\substack{\boldsymbol{y}\in\mathbb{R}^m \\ \boldsymbol{y}\notin\text{null}(B^T)}} \frac{\boldsymbol{y}^T(BA^{-1}B^T + C)\boldsymbol{y}}{\boldsymbol{y}^T\alpha H\boldsymbol{y}}.$$

Under mild assumptions that are certainly met for our problems, $\delta_{\min}$ is bounded away from zero by a constant that depends on the element type but not on the mesh parameter h [7, Section 3.5]. Values of $\delta_{\min}$ are given in Table 3.3 for the cavity problem and the obstacle problem introduced in Section 4.

Tables 3.4 and 3.5 show the bound (3.1) and corresponding value of λ_p for the cavity problem. We see that the bound is pessimistic when $H = \text{diag}(Q)$ (with the exception of Q_1–P_0 elements for which $\text{diag}(Q) = Q$). The bound is similarly pessimistic when $\text{diag}(Q)$ is replaced by the lumped mass matrix $\text{lump}(Q)$, which is unsurprising since $\text{lump}(Q) = 2.25\,\text{diag}(Q)$. However, the bound is very accurate for all three elements when the full pressure mass matrix is used in $\mathcal{P}_\alpha$.

Differences between the values of λ_p for different elements are clearly reflected in differences between the corresponding values of $\delta_{\min}$. Thus, it seems that when H in (1.4) is the full pressure mass matrix, the eigenvalue λ_p is determined mainly by this constant, which varies only mildly between the different element types, and which is bounded away from zero independently of h. Qualitatively similar results are observed for the obstacle problem described in Section 4. Importantly, by examining (3.1) it seems that when H is the pressure mass matrix we can accurately bound λ_p as α increases, which allows us to control the magnitude of this eigenvalue.

3.2. Case II eigenvalues. Although the eigenvalue bound (3.1) is descriptive when we use the full pressure mass matrix in $\mathcal{P}_\alpha$, it is rather pessimistic when the diagonal of the pressure mass matrix is used instead (except for Q_1–P_0 elements). It would be useful to have an alternative means of quantifying λ_p when $H = \text{diag}(Q)$ for

TABLE 3.4
Largest negative eigenvalue (λ_p) of $\mathcal{P}_\alpha^{-1}\mathcal{A}$, and bound (3.1) for the cavity problem, a mesh parameter of 2^{-5} and $H = \mathrm{diag}(Q)$, the diagonal of the pressure mass matrix.

	Q_1–Q_1		Q_2–Q_1	
α	λ_p	Bound	λ_p	Bound
1	-0.25	-0.059	-0.11	-0.031
2	-0.13	-0.03	-0.06	-0.016
3	-0.083	-0.02	-0.041	-0.011
4	-0.063	-0.015	-0.031	-0.0079
5	-0.05	-0.012	-0.025	-0.0063
6	-0.042	-0.01	-0.021	-0.0053
7	-0.036	-0.0089	-0.018	-0.0045
8	-0.031	-0.0078	-0.016	-0.004
9	-0.028	-0.0069	-0.014	-0.0035
10	-0.025	-0.0062	-0.013	-0.0032
20	-0.013	-0.0031	-0.0063	-0.0016
40	-0.0063	-0.0016	-0.0032	-0.0008
60	-0.0042	-0.001	-0.0021	-0.00053
80	-0.0031	-0.00078	-0.0016	-0.0004
100	-0.0025	-0.00062	-0.0013	-0.00032

TABLE 3.5
Largest negative eigenvalue (λ_p) of $\mathcal{P}_\alpha^{-1}\mathcal{A}$, and bound (3.1) for the cavity problem, a mesh parameter of 2^{-5} and $H = Q$, the pressure mass matrix.

	Q_1–Q_1		Q_1–P_0		Q_2–Q_1	
α	λ_p	Bound	λ_p	Bound	λ_p	Bound
1	-0.19	-0.19	-0.2	-0.2	-0.18	-0.18
2	-0.1	-0.1	-0.11	-0.11	-0.095	-0.095
3	-0.071	-0.071	-0.073	-0.073	-0.065	-0.065
4	-0.054	-0.054	-0.055	-0.055	-0.049	-0.049
5	-0.044	-0.044	-0.045	-0.045	-0.04	-0.04
6	-0.037	-0.037	-0.038	-0.038	-0.033	-0.033
7	-0.032	-0.031	-0.032	-0.032	-0.029	-0.029
8	-0.028	-0.028	-0.028	-0.028	-0.025	-0.025
9	-0.025	-0.025	-0.025	-0.025	-0.023	-0.023
10	-0.022	-0.022	-0.023	-0.023	-0.02	-0.02
20	-0.011	-0.011	-0.012	-0.012	-0.01	-0.01
40	-0.0057	-0.0056	-0.0058	-0.0058	-0.0052	-0.0052
60	-0.0038	-0.0038	-0.0039	-0.0039	-0.0034	-0.0034
80	-0.0028	-0.0028	-0.0029	-0.0029	-0.0026	-0.0026
100	-0.0023	-0.0023	-0.0023	-0.0023	-0.0021	-0.0021

Q_1–Q_1 and Q_2–Q_1 elements. The latter case appears to be difficult. However, we see from Table 3.1 that for Q_1–Q_1 elements λ_p behaves like $-0.25/\alpha$. We show in the rest of this section that this is indeed the case, and that this eigenvalue is associated with Case II in Theorem 2.1. Since it is possible to characterize the Case II eigenvalues for the full pressure mass matrix, and for Q_1–P_0 elements, we extend our analysis to these cases for completeness. Although we examine the case $H = \mathrm{diag}(Q)$ here, the same analysis could be performed for the lumped mass matrix $H = \mathrm{lump}(Q)$. This is particularly easy for the Q_1 pressure mass matrices considered here for which $\mathrm{lump}(Q) = 2.25\,\mathrm{diag}(Q)$.

Case II eigenvalues satisfy

$$-C\boldsymbol{y} = \lambda\alpha H\boldsymbol{y}, \quad \boldsymbol{y} \in \mathrm{null}(B^T).$$

Our approach for this analysis is to propose a basis for $\mathrm{null}(B^T)$, and then determine whether these basis vectors are eigenvectors of the generalized problem $(-C, \alpha H)$. To

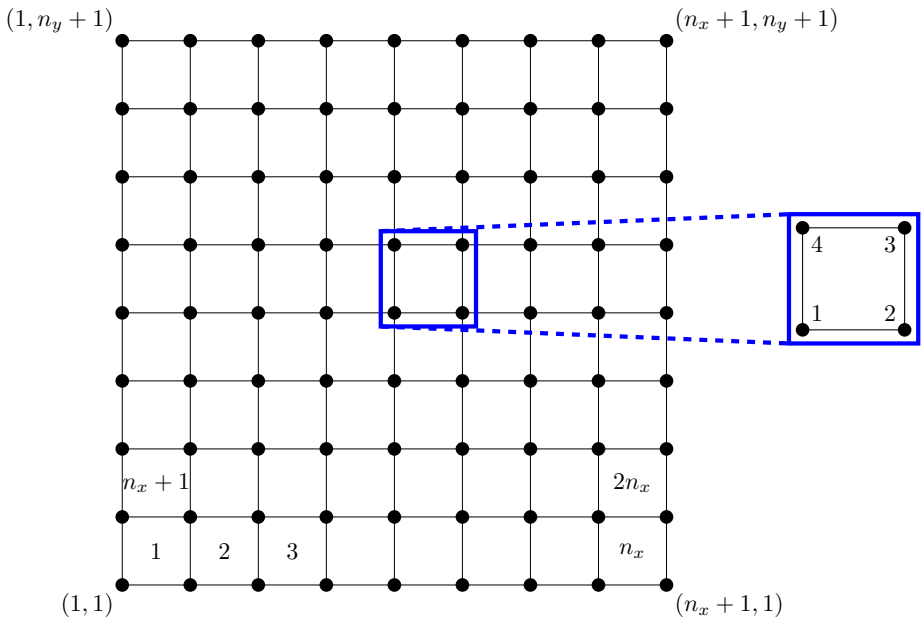

FIG. 3.1. *Diagram of mesh and nodes (left), and node numbering within each element (right).*

do so we require certain notation, and details of the finite element assembly process, that we describe here. We assume that there are n_x elements in the x direction and n_y elements in the y direction, so that the total number of elements is $n_{el} = n_x n_y$. Although we restrict our attention to square domains for simplicity, the same methodology can be used to analyse more complicated domains, as we discuss at the end of this section.

Let $C_k \in \mathbb{R}^{4\times4}$, $Q_k \in \mathbb{R}^{4\times4}$ and $\mathrm{diag}(Q_k) \in \mathbb{R}^{4\times4}$, $k = 1, \ldots, n_{el}$, be the element matrices that are assembled to form C, Q and $\mathrm{diag}(Q)$. Additionally, let $L \in \mathbb{R}^{N\times m}$ be the connectivity matrix that maps local pressure degrees of freedom on element k to the global pressure degrees of freedom $1, \ldots, m$, where $N = 4n_{el}$. Then

$$C = L^T \mathrm{diag}(C_k) L, \quad Q = L^T \mathrm{diag}(Q_k) L, \quad \mathrm{diag}(Q) = L^T \mathrm{diag}(\mathrm{diag}(Q_k)) L. \tag{3.2}$$

We now specify the Q_1–Q_1 connectivity matrix itself. With nodes and elements numbered as in Figure 3.1, each column of L can be succinctly represented using Kronecker products as $\boldsymbol{e}_i \otimes \boldsymbol{e}_j \otimes \boldsymbol{e}_s$, where $\boldsymbol{e}_i \in \mathbb{R}^{n_y}$, $\boldsymbol{e}_j \in \mathbb{R}^{n_x}$ and $\boldsymbol{e}_s \in \mathbb{R}^4$ are the ith, jth and sth unit vectors of the appropriate dimension. The number of elements in a given column depends on whether the corresponding node lies on a corner, a side or in the interior of the domain, and there are nine distinct cases that we now describe.

Consider the (i, j)th node, where the node number is as in Figure 3.1. Then the

corresponding column of L is

$$\ell_k = \begin{cases} \boldsymbol{e}_1 \otimes \boldsymbol{e}_1 \otimes \boldsymbol{e}_1 & i = 1, j = 1, \\ \boldsymbol{e}_1 \otimes \left[\boldsymbol{e}_{i-1} \otimes \boldsymbol{e}_2 + \boldsymbol{e}_i \otimes \boldsymbol{e}_1\right] & i = 2, \ldots, n_x, j = 1, \\ \boldsymbol{e}_1 \otimes \boldsymbol{e}_{n_x} \otimes \boldsymbol{e}_2 & i = n_x + 1, j = 1, \\ \boldsymbol{e}_{j-1} \otimes \boldsymbol{e}_1 \otimes \boldsymbol{e}_4 + \boldsymbol{e}_j \otimes \boldsymbol{e}_1 \otimes \boldsymbol{e}_1 & i = 1, j = 2, \ldots, n_y, \\ \boldsymbol{e}_{j-1} \otimes \left[\boldsymbol{e}_{i-1} \otimes \boldsymbol{e}_3 + \boldsymbol{e}_i \otimes \boldsymbol{e}_4\right] & \\ \quad + \boldsymbol{e}_j \otimes \left[\boldsymbol{e}_{i-1} \otimes \boldsymbol{e}_2 + \boldsymbol{e}_i \otimes \boldsymbol{e}_1\right] & i = 2, \ldots, n_x, j = 2, \ldots, n_y, \\ \boldsymbol{e}_{j-1} \otimes \boldsymbol{e}_{n_x} \otimes \boldsymbol{e}_3 + \boldsymbol{e}_j \otimes \boldsymbol{e}_{n_x} \otimes \boldsymbol{e}_2 & i = n_x + 1, j = 2, \ldots, n_y, \\ \boldsymbol{e}_{n_y} \otimes \boldsymbol{e}_1 \otimes \boldsymbol{e}_4 & i = 1, j = n_y + 1, \\ \boldsymbol{e}_{n_y} \otimes \left[\boldsymbol{e}_{i-1} \otimes \boldsymbol{e}_3 + \boldsymbol{e}_i \otimes \boldsymbol{e}_4\right] & i = 2, \ldots, n_k, j = n_y + 1, \\ \boldsymbol{e}_{n_y} \otimes \boldsymbol{e}_{n_x} \otimes \boldsymbol{e}_3 & i = n_x + 1, j = n_y + 1, \end{cases} \tag{3.3}$$

with $k = (j-1)(n_x+1) + i$, $i = 1, \ldots, n_x + 1$ and $j = 1, \ldots, n_y + 1$. Since L has one element per row,

$$L\mathbf{1}_m = \mathbf{1}_N, \tag{3.4}$$

that is, the connectivity matrix maps the constant vector to one of larger dimension (cf. Lemma 3.2 below).

3.2.1. Q_1–Q_1 elements. We begin with Q_1–Q_1 elements. Following the implementation in the Incompressible Flow & Iterative Solver Software (IFISS) [8, 9, 20], we employ the stabilization approach of Dohrmann and Bochev [6] (see also [7, Section 3.3.2]), who define the stabilization matrix on the kth element to be

$$C_k = Q_k - \boldsymbol{q}\boldsymbol{q}^T|\square_k|, \tag{3.5}$$

where $\boldsymbol{q} = [\frac{1}{4}, \frac{1}{4}, \frac{1}{4}, \frac{1}{4}]^T$ and $|\square_k|$ is the element area. With this choice it follows from (3.2) that the stabilization matrix C satisfies

$$C = L^T \operatorname{diag}(Q_k - \boldsymbol{q}\boldsymbol{q}^T|\square_k|)L = Q - |\square_k|\boldsymbol{w}\boldsymbol{w}^T,$$

where $\boldsymbol{w} = \frac{1}{4}L^T\mathbf{1}_N$. It is straightforward to compute that $\operatorname{null}(C_k) = \operatorname{span}\{\mathbf{1}_4\}$. Since the connectivity matrix maps the constant vector to one of larger dimension (see (3.4)), and C satisfies (3.2), it follows that $\operatorname{null}(C) = \operatorname{span}\{\mathbf{1}_m\}$.

In the Dorhmann and Botchev strategy the Case II eigenvalues satisfy $-C\boldsymbol{y} = \lambda\alpha H\boldsymbol{y}$ with $\boldsymbol{y} \in \operatorname{null}(B^T)$. Without any modifications to B in (1.2) for the incorporation of essential boundary conditions, $\operatorname{null}(B^T) = \operatorname{span}\{\pm\mathbf{1}_{\mathrm{m}}\}$, where $\pm\mathbf{1}$ is the vector of alternating signs, i.e., $(\pm\mathbf{1})_k = (-1)^{k+1}$ [18, 19]. Imposing certain boundary conditions may increase the dimension of $\operatorname{null}(B^T)$.

To show that we have a Case II eigenvalue, we must be able to show that $\pm\mathbf{1}$ is an eigenvector of $-C\boldsymbol{y} = \lambda\alpha \operatorname{diag}(Q)\boldsymbol{y}$ or, equivalently, of

$$\mathbf{0} = L^T(C_k + \lambda\alpha \operatorname{diag}(Q_k))L\boldsymbol{y}.$$

Since the eigenvalues of $(-C, \alpha \operatorname{diag}(Q))$ are closely related to those of $(-C_k, \alpha \operatorname{diag}(Q_k))$, we first determine the eigenvalues and eigenvectors of this small problem.

LEMMA 3.1. *The eigenpairs of* $(-C_k, \alpha \operatorname{diag}(Q_k))$ *are* $(\theta_s, \widetilde{\boldsymbol{v}}_s)$, $s = 1, \ldots, 4$ *where*

$$\Theta = \begin{bmatrix} \theta_1 & & & \\ & \theta_2 & & \\ & & \theta_3 & \\ & & & \theta_4 \end{bmatrix} = \begin{bmatrix} 0 & & & \\ & -\frac{0.25}{\alpha} & & \\ & & -\frac{0.75}{\alpha} & \\ & & & -\frac{0.75}{\alpha} \end{bmatrix}$$

and

$$V = \begin{bmatrix} \widetilde{\boldsymbol{v}}_1 & \widetilde{\boldsymbol{v}}_2 & \widetilde{\boldsymbol{v}}_3 & \widetilde{\boldsymbol{v}}_4 \end{bmatrix} = \begin{bmatrix} 1 & -1 & 1 & 1 \\ 1 & 1 & 1 & -1 \\ 1 & -1 & -1 & -1 \\ 1 & 1 & -1 & 1 \end{bmatrix}.$$

Proof. The result is obtained by straightforward computation. □

The eigenpair $(\theta_2, \widetilde{\boldsymbol{v}}_2)$ seems promising since $\theta_2 = -0.25/\alpha$ matches the observed value of λ_p in Table 3.1, while $\widetilde{\boldsymbol{v}}_2 = \pm\mathbf{1}_4$. To find the corresponding eigenpairs of $(-C, \alpha\,\mathrm{diag}(Q))$ we now extend $\widetilde{\boldsymbol{v}}_s$, $s = 1, \ldots, 4$, to vectors of length m via

$$\boldsymbol{v}_s = (L^T L)^{-1} L^T \widehat{\boldsymbol{v}}_s, \tag{3.6}$$

where

$$\widehat{\boldsymbol{v}}_s = \begin{cases} \mathbf{1}_{n_y} \otimes \mathbf{1}_{n_x} \otimes \widetilde{\boldsymbol{v}}_1 = \mathbf{1} & s = 1, \\ \pm\mathbf{1}_{n_y} \otimes \pm\mathbf{1}_{n_x} \otimes \widetilde{\boldsymbol{v}}_2 = \pm\mathbf{1} & s = 2, \\ \pm\mathbf{1}_{n_y} \otimes \mathbf{1}_{n_x} \otimes \widetilde{\boldsymbol{v}}_3 & s = 3, \\ \mathbf{1}_{n_y} \otimes \pm\mathbf{1}_{n_x} \otimes \widetilde{\boldsymbol{v}}_4 & s = 4. \end{cases} \tag{3.7}$$

Note that

$$\widehat{\boldsymbol{v}}_s = [\epsilon_1 \widetilde{\boldsymbol{v}}_s^T, \epsilon_2 \widetilde{\boldsymbol{v}}_s^T, \ldots, \epsilon_{n_{el}} \widetilde{\boldsymbol{v}}_s^T]^T, \tag{3.8}$$

with $\epsilon_k \in \{-1, 1\}$, $k = 1, \ldots, n_{el}$.

To proceed we require a technical result that shows that the $\widehat{\boldsymbol{v}}_s$ lie in range(L).

LEMMA 3.2. *The vectors $\widehat{\boldsymbol{v}}_s$, $s = 1, \ldots, 4$ in* (3.7) *satisfy $\widehat{\boldsymbol{v}}_s \in \mathrm{range}(L)$.*

Proof. We must be able to combine columns ℓ_p of L in (3.3) to get $\widehat{\boldsymbol{v}}_s$, $s = 1, \ldots, 4$. It is straightforward, although rather cumbersome, to show that

$$\widehat{\boldsymbol{v}}_1 = \sum_{j=1}^{n_y+1} \sum_{i=1}^{n_x+1} \ell_{(j-1)(n_x+1)+i}, \qquad \widehat{\boldsymbol{v}}_2 = \sum_{j=1}^{n_y+1} \sum_{i=1}^{n_x+1} (-1)^{i+j} \ell_{(j-1)(n_x+1)+i},$$

$$\widehat{\boldsymbol{v}}_3 = \sum_{j=1}^{n_y+1} \sum_{i=1}^{n_x+1} (-1)^{i+1} \ell_{(j-1)(n_x+1)+i}, \qquad \widehat{\boldsymbol{v}}_4 = \sum_{j=1}^{n_y+1} \sum_{i=1}^{n_x+1} (-1)^{j+1} \ell_{(j-1)(n_x+1)+i},$$

which proves the result. □

Since $L(L^T L)^{-1} L^T$ is an orthogonal projector onto range(L), a consequence of Lemma 3.2 is that

$$L\boldsymbol{v}_s = L(L^T L)^{-1} L^T \widehat{\boldsymbol{v}}_s = \widehat{\boldsymbol{v}}_s, \quad s = 1, \ldots, 4. \tag{3.9}$$

Importantly, this means that $L\boldsymbol{v}_2 = \widehat{\boldsymbol{v}}_2 = \pm\mathbf{1} \in \mathrm{null}(B^T)$.

The final step is to combine (3.9) with Lemma 3.1 to show that $\widehat{\boldsymbol{v}}_2$ is indeed an eigenvector of $(-C, \alpha\,\mathrm{diag}(Q))$, with corresponding eigenvalue $-0.25/\alpha$.

LEMMA 3.3. *The pairs $(\lambda_s, \boldsymbol{v}_s)$, $s = 1, \ldots, 4$ satisfy $-C\boldsymbol{v}_s = \lambda_s \alpha\,\mathrm{diag}(Q)\boldsymbol{v}_s$, where λ_s are as in Lemma 3.1 and $\boldsymbol{v}_s$ are defined by* (3.6).

Proof. From (3.2) we have that $C\boldsymbol{v}_s+\lambda_s\alpha\,\mathrm{diag}(Q)\boldsymbol{v}_s = L^T(C_k+\lambda_s\alpha\,\mathrm{diag}(Q_k))L\boldsymbol{v}_s$. Thus, using (3.8), (3.9) and Lemma 3.1, we find that

$$\begin{aligned}
&C\boldsymbol{v}_s + \lambda_s\alpha\,\mathrm{diag}(Q_k)\boldsymbol{v}_s \\
&= L^T \begin{bmatrix} C_k + \lambda_s\alpha\,\mathrm{diag}(Q_k) & & & \\ & C_k + \lambda_s\alpha\,\mathrm{diag}(Q_k) & & \\ & & \ddots & \\ & & & C_k + \lambda_s\alpha\,\mathrm{diag}(Q_k) \end{bmatrix} \begin{bmatrix} \epsilon_1\widetilde{\boldsymbol{v}}_s \\ \epsilon_2\widetilde{\boldsymbol{v}}_s \\ \vdots \\ \epsilon_{n_{el}}\widetilde{\boldsymbol{v}}_s \end{bmatrix} \\
&= \boldsymbol{0},
\end{aligned}$$

which shows that $(\lambda_s, \boldsymbol{v}_s)$ are eigenpairs of $(-C, \alpha\,\mathrm{diag}(Q))$. ∎

Returning to Theorem 2.1, we see that the vectors $\boldsymbol{v}_s$, $s = 1, \ldots, 4$ are candidates for $\boldsymbol{y}$ in Case II. However, only $\boldsymbol{v}_2$ lies in $\mathrm{null}(B^T)$ before B is modified to accommodate any essential boundary conditions. Thus, $\lambda = -0.25$ and $\boldsymbol{y} = \boldsymbol{v}_2$ satisfy the conditions for Case II and this is precisely the eigenvalue λ_p that we observe in Table 3.1. Of course, certain boundary conditions may increase the dimension of $\mathrm{null}(B^T)$, in which case $\boldsymbol{v}_1$, $\boldsymbol{v}_3$ and/or $\boldsymbol{v}_4$ may lie in the nullspace of this modified matrix. For example, for the channel problem all four vectors lie in the nullspace.

For completeness we now consider the case where $H = Q$, the pressure mass matrix, which can be analysed in a very similar manner to $H = \mathrm{diag}(Q)$ above. If $-C\boldsymbol{v} = \lambda\alpha Q\boldsymbol{v}$ then $\boldsymbol{0} = L^T(C_k + \lambda\alpha Q_k)L\boldsymbol{v}$. The four eigenpairs of $(-C_k, \alpha Q_k)$ are $(0, \widetilde{\boldsymbol{v}}_1)$ and $(-1/\alpha, \widetilde{\boldsymbol{v}}_s)$, $s = 2, 3, 4$. A result similar to Lemma 3.3 then shows that $(0, \boldsymbol{v}_1)$, $(-1/\alpha, \boldsymbol{v}_s)$, $s = 2, 3, 4$, are eigenpairs of $(-C, \alpha Q)$.

As above, before B is modified to accommodate boundary conditions, $\mathrm{null}(B^T) = \mathrm{span}\{\boldsymbol{v}_2\}$ and the eigenvalue $-1/\alpha$ (with eigenvector $\boldsymbol{v}_2$) is guaranteed to be an eigenvalue of $\mathcal{P}_f^{-1}\mathcal{A}$. However, $\boldsymbol{v}_1$, $\boldsymbol{v}_3$ and/or $\boldsymbol{v}_4$ may lie in the nullspace of the modified matrix. We stress that the difference between this and the diagonal pressure mass matrix approximation is that $\lambda_p \neq -1/\alpha$. Instead λ_p is as in Table 3.2, and is bounded by (3.1).

3.2.2. Q_1–P_0 elements. We now turn our attention to Q_1–P_0 elements which have one pressure degree of freedom per element, located at the element centre. A consequence is that the pressure mass matrix is diagonal, so that $Q = \mathrm{diag}(Q) = |\Box_k|I$, where $|\Box_k|$ is the area of a single element. For these elements B^T has full rank except in the case of Dirichlet boundary conditions, in which case $\mathrm{null}(B^T) = \mathrm{span}\{\boldsymbol{v}_1, \boldsymbol{v}_2\}$ where $\boldsymbol{v}_1$ and $\boldsymbol{v}_2$ are as in (3.7).

The stabilization matrix we choose is that in [7, Section 3.3.2], which we briefly describe here. Consider a macroelement comprising a 2×2 patch of elements. Then the kth macroelement stabilization matrix is

$$C_k = |\Box_k| \begin{bmatrix} 2 & -1 & 0 & -1 \\ -1 & 2 & -1 & 0 \\ 0 & -1 & 2 & -1 \\ -1 & 0 & -1 & 2 \end{bmatrix},$$

$Q_k = |\Box_k|I$, and the connectivity matrix that maps pressure degrees of freedom on a macroelement to global degrees of freedom is the identity, i.e., $L = I$. It is straightforward to compute that (C_k, Q_k) has eigenpairs $(0, \widetilde{\boldsymbol{v}}_1)$, $(4, \widetilde{\boldsymbol{v}}_2)$, $(2, \widetilde{\boldsymbol{v}}_3)$ and $(2, \widetilde{\boldsymbol{v}}_4)$, where $\widetilde{\boldsymbol{v}}_s$, $s = 1, \ldots, 4$ are as in Lemma 3.1. Since

$$C\boldsymbol{v} - \lambda Q\boldsymbol{v} = \mathrm{diag}(C_k - \lambda Q_k)\boldsymbol{v},$$

the results of Section 3.2.1 can be applied to show that $(0, \boldsymbol{v}_1)$, $(4, \boldsymbol{v}_2)$, $(2, \boldsymbol{v}_3)$ and $(2, \boldsymbol{v}_4)$ are all eigenpairs of (C, Q). In fact, because C is block diagonal and Q is diagonal, it is possible to take $\boldsymbol{e}_j \otimes \boldsymbol{v}_s$, $j = 1, \ldots, n_{el}$ as eigenvectors, where $\boldsymbol{e}_j \in \mathbb{R}^{n_{el}}$ is the jth unit vector.

Thus, for problems with purely Dirichlet boundary conditions, $\boldsymbol{v}_1$ and $\boldsymbol{v}_4$ lie in null(B^T), and both $(0, \boldsymbol{v}_4)$ and $(1, \boldsymbol{v}_1)$ are Case II eigenpairs. Otherwise, there are no Case II eigenvalues and all non-unit eigenvalues are described by Case III of Theorem 2.1.

3.3. Discussion. It is clear that the methodology outlined above could be applied to non-square domains to ascertain the presence of Case II eigenvalues, although it may be more difficult to determine the appropriate nullspace vectors [18], and the connectivity matrix may be more complicated to describe.

As an example of what we might expect for more general domains, we performed numerical experiments for the L-shaped domain of the backward-facing step problem in IFISS (see Section 3.1 of [7] for a full problem description). We numerically verified that when Q_1–Q_1 elements are used, $(-C, \alpha\,\mathrm{diag}(Q))$ has eigenpairs $(0, \boldsymbol{v}_1)$, $(-0.25/\alpha, \boldsymbol{v}_2)$, $(-0.75/\alpha, \boldsymbol{v}_3)$ and $(-0.75/\alpha, \boldsymbol{v}_4)$, while $(-C, \alpha Q)$ has eigenpairs $(0, \boldsymbol{v}_1)$ and $(-1/\alpha, \boldsymbol{v}_s)$, $s = 2, 3, 4$, i.e., the same eigenpairs as for the square domain. Since $\boldsymbol{v}_2 \in$ null(B^T), $-0.25/\alpha$ is a Case II eigenvalue. Moreover, after boundary conditions are applied we find that $(-0.75/\alpha, \boldsymbol{v}_4)$ is an additional Case II eigenvalue. For Q_1–P_0 elements we find that $(0, \boldsymbol{v}_1)$, $(-4/\alpha, \boldsymbol{v}_2)$, $(-2/\alpha, \boldsymbol{v}_3)$ and $(-2/\alpha, \boldsymbol{v}_4)$ are eigenpairs of $(-C, \alpha Q)$. However, because this problem has a natural outflow condition there are no Case II eigenpairs. We note that exactly the same results hold for the obstacle problem described in the next section.

We conclude this section by summarizing the results obtained thus far. We have found that increasing the parameter α in $\mathcal{P}_\alpha$ results in more clustered eigenvalues of $\mathcal{P}_\alpha^{-1}\mathcal{A}$ when solving a range of Stokes problems, and the eigenvalues of the preconditioned system do not rapidly approach zero as α is raised. We therefore recommend that a moderate scaling parameter is incorporated into a preconditioner for the Stokes equations. In the next section we will justify this experimentally.

4. Numerical verification. Having motivated the application of scaled saddle-point preconditioners to Stokes problems, we would like to demonstrate the effect of such preconditioners on various test problems. To do this we run the preconditioned MINRES algorithm within the IFISS software system [8, 9, 20] in MATLAB. In particular, we examine the regularized cavity flow from Section 3, as well as an obstacle flow problem. The latter problem is posed on the channel $\Omega = [0, 8] \times [-1, 1]$ with the square obstacle $[\frac{7}{4}, \frac{9}{4}] \times [-\frac{1}{4}, \frac{1}{4}]$ removed (see Figure 4.2). No-flow conditions are applied at the top and bottom walls, and at the obstacle boundary. We impose a Poiseuille flow condition, that is $v_x = 1 - y^2$, $v_y = 0$, on the inflow boundary; we also specify a natural boundary condition on the outflow boundary. In Figures 4.1 and 4.2, we provide streamline plots for the velocity solutions of these problems, as well as plots for the pressure solutions.

In Table 4.1 we present iteration numbers for the MINRES solution of the regularized cavity problem using stabilized Q_1–Q_1 elements on a uniform mesh, with a preconditioned residual norm tolerance of 10^{-6}. Within the preconditioner, we use one algebraic multigrid (AMG) V-cycle with point damped Gauss-Seidel smoothing for the matrix $\widehat{A}$, and 10 steps of Chebyshev semi-iteration [11, 12, 26] for H. We present results for different values of the (uniform) mesh parameter h, as well as values

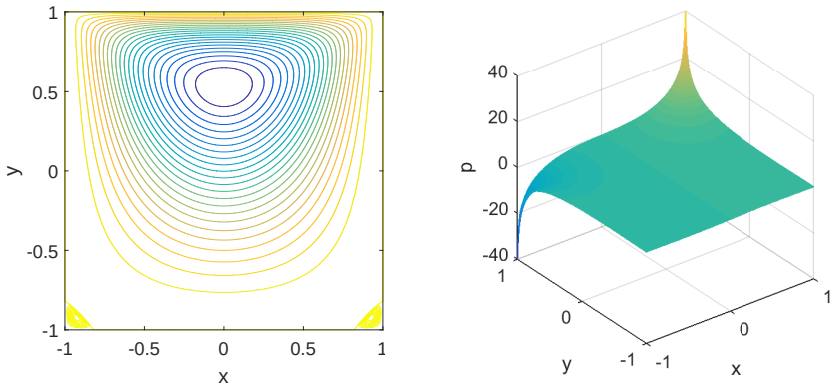

(a) Velocity $\vec{v}$ (b) Pressure p

FIG. 4.1. *Solution plots of velocity $\vec{v}$ and pressure p for the regularized cavity problem.*

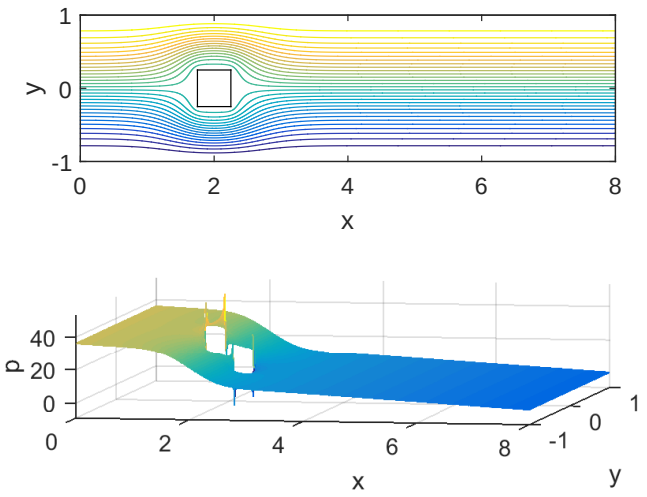

FIG. 4.2. *Solution plots of velocity $\vec{v}$ (top) and pressure p (bottom) for the obstacle flow problem.*

of α within $\mathcal{P}_\alpha$. We observe that when α is increased, the iteration numbers clearly decrease, and there is hence a considerable benefit to applying the scaled preconditioner. This is observed for all values of mesh parameter tested.

In Table 4.3 we present iteration numbers for the solution of the obstacle problem for a range of finite element discretizations, and a range of preconditioning strategies as presented in Table 4.2. The matrix $\widehat{A}$ is either taken to be A or an AMG V-cycle applied to it; the preconditioner H for the Schur complement is either the diagonal of Q or 10 steps of Chebyshev semi-iteration applied to Q. We highlight that we also ran the same tests with $H = Q$, and obtained very similar results as when using Chebyshev semi-iteration. When Q_1–P_0 finite elements are used, Q is diagonal, so we only run the tests for preconditioner options 1 and 3. In all cases the mesh parameter is fixed as $h = 2^{-8}$, and different values of α are again taken within $\mathcal{P}_\alpha$. We see that applying Chebyshev semi-iteration within the Schur complement approximation results in faster convergence than a diagonal approximation; using AMG to approximate the $(1,1)$-

TABLE 4.1
Results for the cavity problem solved with Q_1–Q_1 finite elements, for a range of values of h and α.

	h						
α	2^{-2}	2^{-3}	2^{-4}	2^{-5}	2^{-6}	2^{-7}	2^{-8}
1	21	31	35	38	40	41	43
2	18	27	30	33	35	36	37
3	18	25	29	31	33	34	36
4	18	25	28	30	32	33	34
5	17	23	28	30	31	33	33
6	17	23	28	30	30	33	33
7	17	23	28	29	31	31	33
8	17	22	26	29	31	32	32
9	17	22	26	29	31	32	32
10	17	22	26	29	31	32	33
20	17	22	27	28	29	31	32
40	17	23	26	29	30	33	32
60	16	23	27	30	31	32	33
80	16	24	28	29	32	33	34
100	16	24	28	29	32	34	32

block yields roughly similar convergence as an exact inverse for Q_1–Q_1 elements, but higher iteration counts for Q_1–P_0 and Q_2–Q_1 elements. Significantly, we once again observe the advantage of increasing α within the preconditioner—this behavior is replicated for all preconditioning options tested when stabilized finite elements are used.

TABLE 4.2
Different preconditioner options.

	Preconditioner
1	Full A, Diagonal of Q
2	Full A, Chebyshev semi-iteration for Q
3	AMG for A, Diagonal of Q
4	AMG for A, Chebyshev semi-iteration for Q

TABLE 4.3
Results for the obstacle flow problem with $h = 2^{-7}$ for different preconditioners, and for a range of α and element types.

	Q_1–Q_1				Q_1–P_0		Q_2–Q_1			
α	1	2	3	4	1	3	1	2	3	4
1	64	67	67	72	69	77	77	49	89	61
2	61	60	65	64	62	70	75	48	86	60
3	61	55	65	60	59	67	73	48	85	60
4	59	54	63	59	58	66	73	49	83	59
5	59	53	63	57	58	65	71	47	84	60
6	58	52	63	58	56	64	71	47	82	60
7	58	52	63	58	56	64	71	47	83	61
8	57	51	62	57	56	65	70	47	83	61
9	57	51	62	57	55	64	70	47	82	60
10	56	50	62	57	55	64	70	47	82	60
20	56	49	62	59	53	65	68	46	83	62
40	54	48	64	61	52	68	66	45	84	66
60	54	47	65	63	52	69	65	45	87	67
80	52	47	66	64	52	71	65	45	88	69
100	52	47	66	66	52	72	63	45	90	70

5. Concluding remarks. This work shows that including a simple scaling to well-established block diagonal preconditioners for Stokes problems can result in significantly faster convergence when applying the preconditioned MINRES method. We demonstrated theoretically why this occurs by analyzing the eigenvalues of the preconditioned matrix $\mathcal{P}_\alpha^{-1}\mathcal{A}$. In particular, the positive eigenvalues cluster near 1 as the scaling parameter is increased, with the negative eigenvalues also clustering and only approaching 0 slowly. We also show that the performance gains can be significant (30% reduction in CPU times) if a stabilized mixed approximation method is in use.

Acknowledgements. JWP gratefully acknowledges support from the Engineering and Physical Sciences Research Council (EPSRC) Fellowship EP/M018857/1. JP gratefully acknowledges support from the EPSRC grant EP/I005293.

REFERENCES

[1] O. Axelsson and M. Neytcheva. Eigenvalue estimates for preconditioned saddle point matrices. *Numer. Linear Alg. Appl.*, 13:339–360, 2006.
[2] M. Benzi, G. H. Golub, and J. Liesen. Numerical solution of saddle point problems. *Acta Numer.*, 14:1–137, 2005.
[3] M. Benzi and V. Simoncini. On the eigenvalues of a class of saddle point matrices. *Numer. Math.*, 103:173–196, 2006.
[4] D. Boffii, F. Brezzi, and M. Fortin. *Mixed Finite Element Methods and Applications*. Springer, 2013.
[5] E. Dean and R. Glowinski. On some finite element methods for the numerical solution of incompressible viscous flow. In M. Gunzburger and R. Nicolaides, editors, *Incompressible Computational Fluid Dynamics*, 1993.
[6] C. Dohrmann and P. Bochev. A stabilized finite element method for the Stokes problem based on polynomial pressure projection. *Int. J. Numer. Methods Fluids*, 46:183–201, 2004.
[7] H. Elman, D. Silvester, and A. Wathen. *Finite Elements and Fast Iterative Solvers with Applications in Incompressible Fluid Dynamics, Second Edition*. Oxford University Press, 2014.
[8] H. C. Elman, A. Ramage, and D. J. Silvester. Algorithm 866: IFISS, a Matlab toolbox for modelling incompressible flow. *ACM Trans. Math. Softw.*, 33:2–14, 2007.
[9] H. C. Elman, A. Ramage, and D. J. Silvester. IFISS: a computational laboratory for investigating incompressible flow problems. *SIAM Review*, 56:261–273, 2014.
[10] B. Fischer, A. Ramage, D. J. Silvester, and A. J. Wathen. Minimum residual methods for augmented systems. *BIT Numer. Math.*, 38:527–543, 1998.
[11] G. H. Golub and R. S. Varga. Chebyshev semi-iterative methods, successive over-relaxation iterative methods, and second order Richardson iterative methods. I. *Numer. Math.*, 3:147–156, 1961.
[12] G. H. Golub and R. S. Varga. Chebyshev semi-iterative methods, successive over-relaxation iterative methods, and second order Richardson iterative methods. II. *Numer. Math.*, 3:157–168, 1961.
[13] Y. A. Kuznetsov. Efficient iterative solvers for elliptic finite element problems on nonmatching grids. *Russ. J. Numer. Anal. M.*, 10:187–211, 1995.
[14] J. Liesen and Z. Strakoš. *Krylov Subspace Methods: Principles and Analysis*. Oxford University Press, 2013.
[15] M. F. Murphy, G. H. Golub, and A. J. Wathen. A note on preconditioning for indefinite linear systems. *SIAM J. Sci. Comput.*, 21:1969–1972, 2000.
[16] S. Rhebergen, G. N. Wells, R. F. Katz, and A. J. Wathen. Analysis of block-preconditioners for models of coupled magma/mantle dynamics. *SIAM J. Sci. Comput.*, 36:A1960–A1977, 2014.
[17] T. Rusten and R. Winther. A preconditioned iterative method for saddlepoint problems. *SIAM J. Matrix Anal. Appl.*, 13:887–904, 1992.
[18] R. L. Sani, P. M. Gresho, R. L. Lee, and D. F. Griffiths. The cause and cure (!) of the spurious pressures generated by certain FEM solutions of the incompressible Navier-Stokes equations: Part I. *Int. J. Numer. Methods Fluids*, 1:17–43, 1981.
[19] R. L. Sani, P. M. Gresho, R. L. Lee, D. F. Griffiths, and M. Engelman. The cause and cure

(!) of the spurious pressures generated by certain FEM solutions of the incompressible Navier-Stokes equations: Part II. *Int. J. Numer. Methods Fluids*, 1:171–204, 1981.

[20] D. Silvester, H. Elman, and A. Ramage. Incompressible Flow and Iterative Solver Software (IFISS) version 3.4, August 2015. `http://www.manchester.ac.uk/ifiss/`.

[21] D. Silvester and A. Wathen. Fast iterative solution of stabilised Stokes systems. Part II: Using general block preconditioners. *SIAM J. Numer. Anal.*, 31:1352–1367, 1994.

[22] S. Turek. *Efficient Solvers for Incompressible Flow Problems: An Algorithmic and Computational Approach*. Lecture Notes in Computational Science and Engineering. Springer Berlin Heidelberg, 2012.

[23] R. S. Varga. *Matrix Iterative Analysis*. Prentice Hall, London, 1962.

[24] A. Wathen and D. Silvester. Fast iterative solution of stabilised Stokes systems. Part I: Using simple diagonal preconditioners. *SIAM J. Numer. Anal.*, 30:630–649, 1993.

[25] A. J. Wathen, B. Fischer, and D. J. Silvester. The convergence rate of the minimum residual method for the Stokes problem. *Numer. Math.*, 71:121–134, 1995.

[26] A. J. Wathen and T. Rees. Chebyshev semi-iteration in preconditioning for problems including the mass matrix. *Electron. Trans. Numer. Anal.*, 34:125–135, 2009.